

Supplementary Information

High-Throughput Discovery of $\text{Li}_3\text{Sc}_2(\text{PO}_4)_3$ as a Protective Coating for Stabilizing Mid-Ni NCM Interfaces in All-Solid-State Batteries

Ji Hoon Kim,¹ Seunghyun Lee^{2,3,4,*} and Sang Uck Lee^{1*}

¹School of Chemical Engineering, Sungkyunkwan University, Suwon 16419, Republic of Korea

²Department of Applied Chemistry, Hanyang University ERICA, Ansan 15588, Republic of Korea.

³ Center for Bionano Intelligence Education and Research, Hanyang University ERICA, Ansan 15588, Republic of Korea.

⁴ Department of Energy and Bio Sciences, Hanyang University ERICA, Ansan 15588, Republic of Korea.

* indicates the corresponding author

* Corresponding author: Seunghyun Lee, Sang Uck Lee

Tel.: +82-31-290-7343

E-mail address: leeshyun@hanyang.ac.kr and suleechem@skku.edu

Supporting figures and notes

Ionic conductivity calculation

To obtain the Li-ion diffusivity, we should have Mean-Squared Displacement (MSD). The MSD of mobile ions can be calculated from the average displacements over time duration t , where $r_i(t)$ is the position of a mobile ion.

$$MSD = \frac{1}{N} \sum_i \langle [r_i(t + t_0)]^2 - [r_i(t_0)]^2 \rangle \quad (\text{eq1})$$

The diffusivity (D) can be calculated the movement of mobile ions per time from trajectories generated as a result of AIMD simulations.

$$D = \frac{1}{2dt} MSD \quad (\text{eq2})$$

We can calculate the Li-ion diffusivity of specific temperature because ion diffusivity follows an Arrhenius relationship in no phase transition solid. After attaining each diffusivity of calculated temperatures, we extrapolated the Li-ion diffusivity of specific temperature from an Arrhenius fitting using equation (3).

$$D = D_0 \exp\left(-\frac{E_a}{kT}\right) \quad (\text{eq3})$$

Here, D_0 is diffusivity at infinite temperature, E_a is the activation energy of diffusion, k is the Boltzmann constant and T is the calculated temperature. E_a can calculate from the linear fitting of $\log(D)$ versus $1/T$. The ionic conductivity σ_T of a specific temperature can be obtained using the Li-ion diffusivity of specific temperatures from the Nernst-Einstein relation:

$$\sigma_T = \frac{\rho z^2 F^2}{RT} D_T \quad (\text{eq4})$$

where ρ is the molar density of mobile ions in a unit cell, z is the charge of mobile ions, F is Faraday's constant, R is the gas constant, T is temperature and D_T is the Li-ion diffusivity of a specific temperature.

Electrochemical stability window calculation

The electrochemical stability window was determined using a methodology consistent with previous first-principles studies on solid-state electrolytes (SSEs).^{1, 2} In this approach, electrochemical stability is evaluated by examining the phase behavior of the material under different lithium chemical potentials (μ_{Li}), which correspond to a range of electrode voltage. To quantify this, we constructed grand potential phase diagrams at 0 K, which describe the thermodynamic stability of each compound in contact with lithium at a given chemical potential. For a given composition c , the grand potential Φ is defined as:

$$\Phi[c, \mu_{Li}] = E[c] - n_{Li}[c] \cdot \mu_{Li} \quad (\text{eq5})$$

where $E[c]$ is the DFT total energy of compound c , $n_{Li}[c]$ is the Li concentration of composition c . Phase stability is then evaluated by determining whether the compound lies on the lower convex hull of the grand potential diagram across a range of values (0 to -5 eV, corresponding to 0-7 V vs. Li/Li⁺). Compounds that remain on the convex hull across a range of μ_{Li} are considered stable within that interval. The upper and lower of this interval (μ_{ox}, μ_{red}) define the electrochemical stability window, which is converted to voltage using:

$$V_{red} = \frac{\mu_{Li}^0 - \mu_{red}}{e} \quad (\text{eq6})$$

$$V_{ox} = \frac{\mu_{Li}^0 - \mu_{ox}}{e} \quad (\text{eq7})$$

where μ_{Li}^0 is the chemical potential of lithium metal and e is the elementary charge.

Chemical mixing reaction energy calculation

To evaluate the chemical compatibility between coating materials and SSEs or cathode interfaces, we calculated the chemical mixing reaction energy (ΔE_{mix}).³ This thermodynamic descriptor quantifies the driving force for interfacial chemical reactions and indicates whether a spontaneous reaction is expected upon contact.

For two reactant phases A and B , the reaction energy was determined by identifying the most stable combination of reaction products that could form from their mixture. The mixing ratio $x \in [0, 1]$ was varied continuously, and the most favorable product configuration was obtained by minimizing the reaction energy:

$$\Delta E_{mix} = \min_{x \in [0,1]} \{E_{pd}[xc_A + (1-x)c_B] - xE[c_A] - (1-x)E[c_B]\} \quad (\text{eq8})$$

Here, c_A and c_B are the atomic compositions of materials A and B , normalized by the total number of atoms; $E[c_A]$ and $E[c_B]$ are their DFT total energies; and $E_{pd}[c]$ is the energy of the most stable decomposition phase (i.e., the convex hull energy) at composition c . The resulting ΔE_{mix} is expressed in units of eV/atom. A large negative ΔE_{mix} represents a strong thermodynamics tendency for reaction at the interface, potentially leading to the formation of electronically insulating or ion-blocking layers. Conversely, a value close to 0 suggests chemical compatibility.

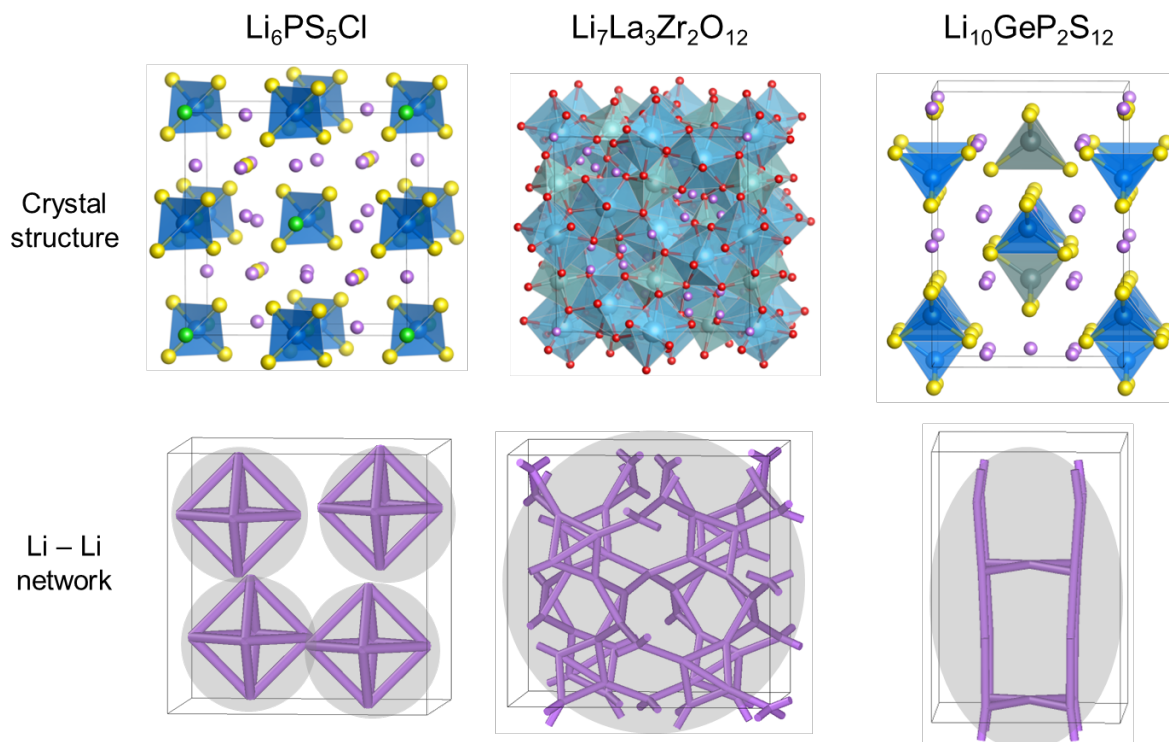


Figure S2. Representative solid-state electrolyte crystal structures (top) with high ionic conductivity and corresponding Li – Li connectivity networks (bottom): $\text{Li}_6\text{PS}_5\text{Cl}$, $\text{Li}_7\text{La}_3\text{Zr}_2\text{O}_{12}$, and $\text{Li}_{10}\text{GeP}_2\text{S}_{12}$. The Li–Li network is visualized to distinct ion transport pathway formed by Li–Li connections ($\leq 3.5 \text{ \AA}$)

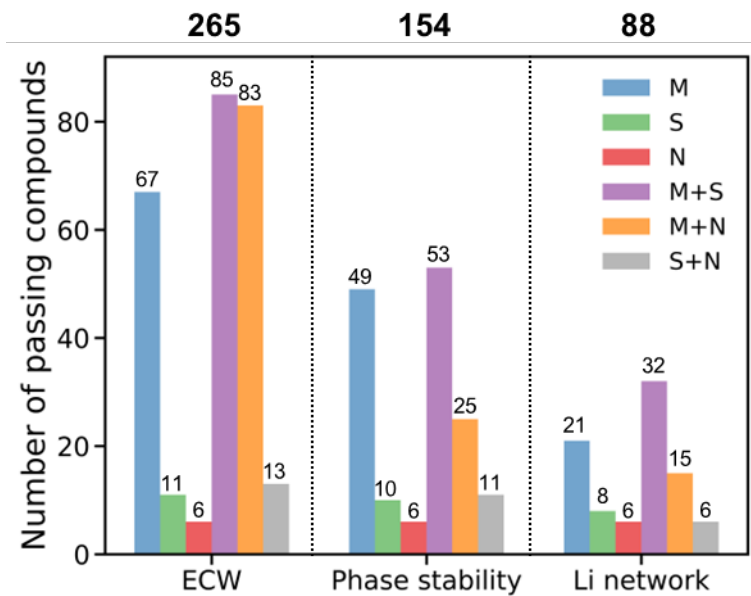


Figure S3. Histogram showing the number of candidates in each elemental category that pass through each filtering step in the high-throughput screening process. Blue, green, red, purple, orange, and gray bars represent materials containing metal (M), semi-metal (S), non-metal (N), metal + semi-metal (M+S), metal + non-metal (M+N), and semi-metal + non-metal (S+N), respectively, excluding Li and O.

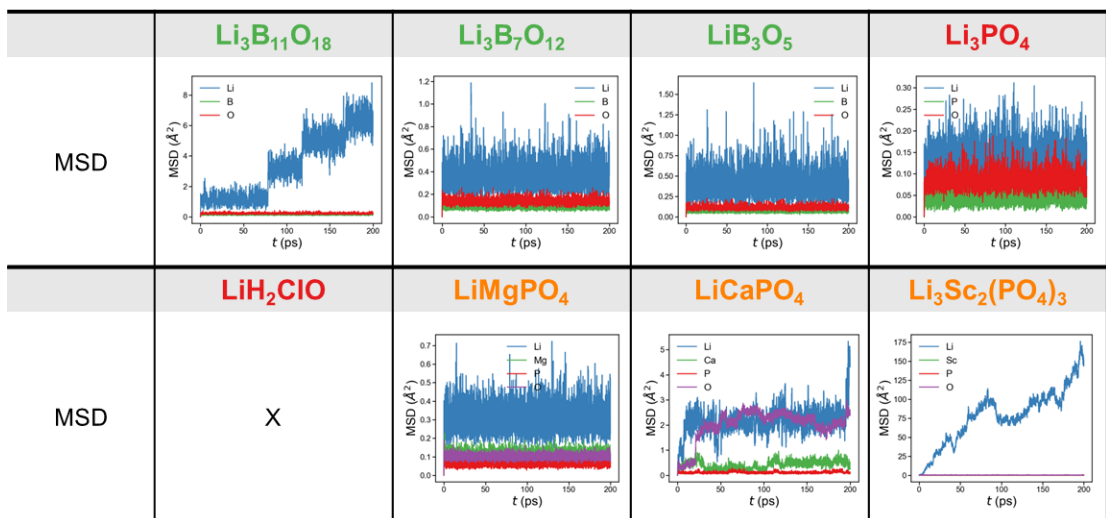


Figure S4. Mean squared displacement (MSD) of Li and framework atoms for 8 representative crystal structures, obtained from AIMD simulations during 200 ps at 1000 K. LiH_2ClO was excluded from the evaluation due to the detachment of H from H_2O .

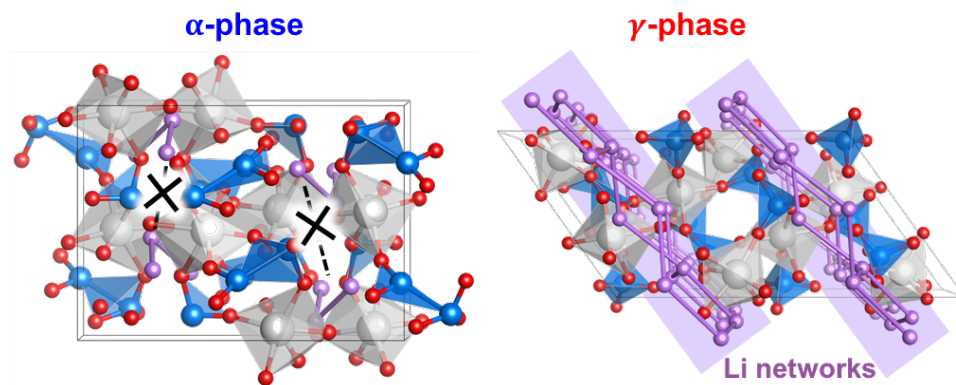


Figure S5. Li-ion networks pathway in two crystal structures for α - and γ -phases. The purple shaded regions highlight Li–Li networks within 3.5 Å.

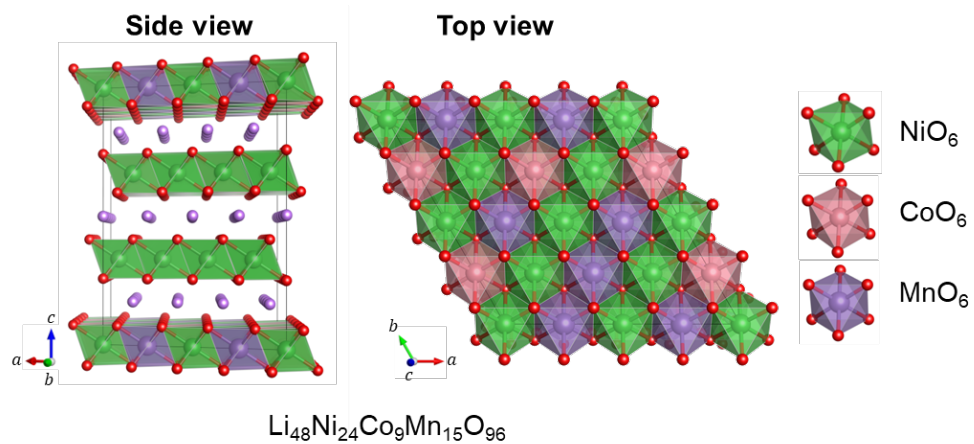


Figure S6. Crystal structure of $\text{LiNi}_{0.5}\text{Co}_{0.2}\text{Mn}_{0.3}\text{O}_2$ (NCM523) used in this study for molecular dynamics simulations, according to viewing perspective.

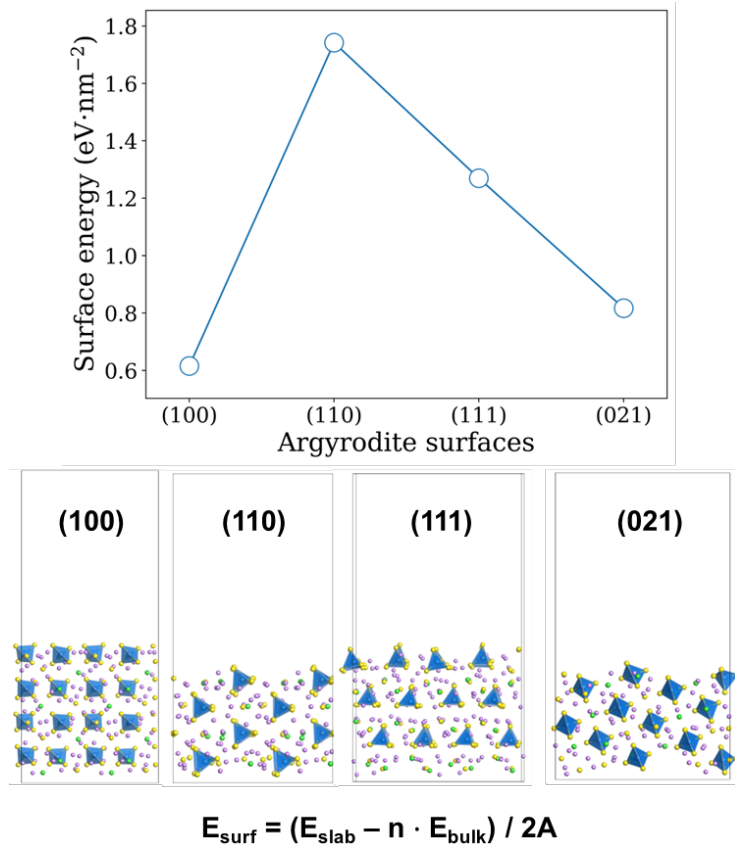


Figure S7. Calculated surface energies and models of Li₆PS₅Cl according to its surface indices.

Table S1. Representative 88 crystal structures screened in high-throughput screening process along with their database source, electrochemical window, interfacial stability, band gap, number of Li–Li networks, and max number of containing Li. Each category represents metal (M), semi-metal (S), non-metal (N), metal + semi-metal (M+S), metal + non-metal (M+N), and semi-metal + non-metal (S+N), respectively, excluding Li and O.

<i>Composition</i>	<i>Category</i>	<i>mp-ID</i>	<i>v1</i>	<i>v2</i>	<i>ECW</i>	ΔE_{rxn} <i>NCM523</i>	ΔE_{rxn} <i>LPSC</i>	<i>Band gap</i>	<i>Li networks</i>	<i>Max number of Li</i>
			(V)	(V)	(V)	(meV /atom)	(meV /atom)	(eV)	(count)	(count)
<i>Li₂BaTi₆O₁₄</i>	M	558083	1.47	3.85	2.38	-7.56	-68.35	2.94	4	2
<i>Li₃SrTa₂O₇</i>	M	558054	1.09	3.55	2.46	0	-52.59	2.27	1	4
<i>Li₂CaTa₂O₇</i>	M	1194523	1.05	3.57	2.52	0	-50.15	2.81	2	4
<i>Li₂TiO₃</i>	M	2931	0.50	3.68	3.18	0	-60.12	3.03	1	8
<i>Li₃TaO₄</i>	M	3151	0.55	3.57	3.02	0	-47.80	4	1	12
<i>Li₃NbO₄</i>	M	31488	0.96	3.60	2.65	0	-96.12	3.84	1	12
<i>Li₄Ti₅O₁₂</i>	M	685194	1.74	3.68	1.94	-15.43	-64.44	2.72	1	8
<i>Li₂Ti₄O₉</i>	M	772151	1.74	3.68	1.94	-17.62	-65.98	2.89	2	2
<i>Li₂Ti₃O₇</i>	M	1190132	1.74	3.68	1.94	-16.45	-65.10	2.98	1	4
<i>LiNdTiO₄</i>	M	10520	0.55	3.54	2.99	0	-78.02	2.28	1	2
<i>Li₁₅Ti₁₁Nb₅O₄₂</i>	M	767393	1.82	3.68	1.87	-11.68	-82.74	2.27	2	4

<i>LiLaTiO₄</i>	M	6521	0.50	3.53	3.03	-78.45	-81.32	2.26	1	2
<i>Li₂Ti₂O₅</i>	M	756294	1.74	3.68	1.94	-7.84	-63.55	3.80	1	4
<i>Li₇Ti₁₂Nb O₃₀</i>	M	767146	1.82	3.68	1.87	-10.84	-71.19	2.62	1	2
<i>Li₄Ti₉O₂₀</i>	M	772090	1.74	3.68	1.94	-11.95	-66.30	3.13	2	4
<i>Li₁₀Ti₁₁Nb ₆O₄₂</i>	M	767498	1.82	3.68	1.87	0	-88.70	2.19	1	2
<i>Li₄Ti₁₁O₂₄</i>	M	766548	1.74	3.68	1.94	0	-66.77	2.57	1	3
<i>Li₄Ba₄Ti₁₉ O₄₄</i>	M	762032	1.75	3.85	2.10	-1.43	-72.60	2.33	1	3
<i>Li₇Ti₇Nb₅ O₃₀</i>	M	767392	1.82	3.68	1.87	0	-98.34	2.12	1	2
<i>Li₄Ti₃O₈</i>	M	755266	1.74	3.68	1.94	0	-62.23	2.17	1	4
<i>Li₃Ta₇O₁₉</i>	M	772220	1.59	3.93	2.34	-21.46	-45.05	2.87	2	3
<i>Li₂Si₂O₅</i>	S	4117	1.26	3.77	2.50	-14.85	0	5.15	1	4
<i>Li₂SiO₃</i>	S	5012	0.76	3.72	2.96	0	0	5.08	1	4
<i>Li₃B₁₁O₁₈</i>	S	1020014	1.93	4.41	2.48	-28.29	0	5.68	2	2
<i>Li₃B₇O₁₂</i>	S	16828	1.30	4.22	2.92	-11.70	0	5.70	2	3
<i>LiBO₂</i>	S	14232	1.07	3.66	2.59	0	0	7.28	1	2
<i>Li₂B₄O₇</i>	S	4779	1.29	3.66	2.37	-10.78	0	5.81	2	4
<i>Li₂Si₃O₇</i>	S	555899	1.32	3.77	2.45	-18.55	0	5.36	2	4
<i>LiB₃O₅</i>	S	3660	1.93	4.22	2.29	-21.15	0	6.48	2	2

<i>Li₃PO₄</i>	N	13725	0.69	4.19	3.51	0	0	5.82	1	6
<i>Li₂SO₄</i>	N	4556	1.63	4.65	3.02	0	-99.22	6.01	1	8
<i>Li₂CO₃</i>	N	3054	1.27	4.09	2.82	0	-83.80	5.06	1	4
<i>LiH₂BrO</i>	N	754153	1.55	3.68	2.12	-5.62	0	4.31	1	4
<i>Li₂H₂SO₅</i>	N	23849	1.99	4.40	2.41	0	-90.79	5.58	1	4
<i>LiH₂ClO</i>	N	760502	1.54	4.07	2.53	0	-22.15	5.31	1	4
<i>LiTmSiO₄</i>	M+S	15066	0.84	3.65	2.81	0	0	4.87	2	2
<i>LiYSiO₄</i>	M+S	558941	0.74	3.61	2.87	0	-46.01	5.27	2	2
<i>LiScSiO₄</i>	M+S	6224	1.08	3.77	2.70	-3.15	0	4.61	2	2
<i>Li₂TiSiO₅</i>	M+S	6332	1.47	3.81	2.34	-7.0	0	3.22	1	4
<i>LiSrBO₃</i>	M+S	10814	0.32	3.54	3.23	0	-95.69	4.36	2	2
<i>LiKSi₂O₅</i>	M+S	558102	1.05	3.80	2.75	-6.02	0	4.71	1	2
<i>Li₃AlSiO₅</i>	M+S	1020023	0.64	3.62	2.98	0	0	4.94	1	12
<i>Li₂BeSiO₄</i>	M+S	8070	0.50	3.87	3.37	0	0	6.06	1	4
<i>Li₃Gd(BO₃)₂</i>	M+S	559706	0.78	3.52	2.74	0	-57.90	3.18	2	6
<i>Li₂MgSiO₄</i>	M+S	11189	0.52	3.71	3.20	0	0	4.76	1	8
<i>Li₆Tm(BO₃)₃</i>	M+S	1211340	0.88	3.51	2.63	0	-49.85	4.80	1	24
<i>LiKB₄O₇</i>	M+S	6648	1.16	3.74	2.58	-2.83	0	5.34	4	2

<i>LiRbB₄O₇</i>	M+S	6787	1.13	3.73	2.60	-2.77	0	5.14	4	2
<i>Li₄Ca(BO₃)₂</i>	M+S	557467	0.40	3.50	3.10	0	-73.07	4.73	2	4
<i>Li₄Cs₃(BO₃)₇</i>	M+S	1019615	0.91	3.59	2.68	0	-48.71	4.53	3	4
<i>Li₃Sc(BO₃)₂</i>	M+S	557012	0.95	3.56	2.61	0	-51.53	4.52	1	6
<i>Li₄Cs(BO₂)₅</i>	M+S	1019716	0.96	3.57	2.61	0	0	4.66	2	8
<i>Li₃Cs₂(BO₃)₇</i>	M+S	1019607	0.96	3.57	2.61	0	0	4.53	2	4
<i>Li₆Rb₅(BO₃)₁₁</i>	M+S	1020620	0.98	3.52	2.54	0	-59.13	4.51	1	6
<i>Li₃Cs₂(BO₃)₅</i>	M+S	966802	0.96	3.57	2.61	0	-48.20	4.54	2	3
<i>Li₃Rb₂(BO₃)₇</i>	M+S	1020664	1	3.54	2.54	0	0	4.63	2	4
<i>Li₂Ca₂Si₅O₁₃</i>	M+S	560247	1.32	3.77	2.45	-14.52	0	4.94	1	4
<i>Li₂Ca₂Si₂O₇</i>	M+S	1020009	0.81	3.56	2.74	0	-66.21	4.74	6	2
<i>LiBeBO₃</i>	M+S	1020026	1.07	3.66	2.59	-2.40	0	6.08	1	2
<i>Li₂AlBO₄</i>	M+S	556655	1.02	3.67	2.66	0	0	5.03	1	8
<i>Li₃Al(SiO₄)₂</i>	M+S	1222486	0.76	3.62	2.86	0	0	4.56	1	5
<i>Li₂Mg₂Si₄O₁₁</i>	M+S	561336	1.32	3.77	2.45	-16.81	0	5.13	2	2
<i>Li₃Al(BO₃)₂</i>	M+S	6097	1.07	3.66	2.59	0	0	4.82	1	6
<i>Li₂Al₂SiO₆</i>	M+S	1222720	1.10	3.68	2.58	0	0	4.63	1	2
<i>Li₂Ti(BO₃)₂</i>	M+S	759926	1.74	3.68	1.94	0	-42.51	2.95	2	4

Li_2MgSi_5 O_{12}	M+S	1222909	1.32	3.77	2.45	0	-8.86	5.16	2	4
$Li_3Co(BO_2)_5$	M+S	768669	1.91	3.66	1.75	0	-39.91	3.05	2	4
$Li_2Ta_2(OF_2)_3$	M+N	561011	1.70	4.83	3.13	-57.34	-62.46	3.84	3	2
$Li_3Sc_2(PO_4)_3$	M+N	6565	1.86	4.19	2.33	-37.30	-24.69	4.76	2	6
$LiMgPO_4$	M+N	9625	1.58	4.18	2.61	-20.62	0	5.43	2	2
Li_2NaPO_4	M+N	558045	0.71	3.99	3.29	0	0	5.34	2	4
$LiMnPO_4$	M+N	18997	1.88	3.78	1.90	-64.81	-52.25	3.41	2	2
$LiNa_5(PO_4)_2$	M+N	559452	0.73	3.89	3.15	0	-74.06	4.52	4	2
$LiCaPO_4$	M+N	16804	1.17	4.08	2.91	0	-28.06	5.18	2	3
$Li_3V(H_6O_5)_2$	M+N	1193122	1.88	3.94	2.06	0	-90.80	4.07	1	3
$Li_4Mn(PO_4)_2$	M+N	26081	1.88	3.78	1.90	-44.07	0	4.13	1	16
$Li_3Na_5Ti_5$ O_{14}	M+N	774609	1.40	3.60	2.20	0	-96.10	3.14	1	3
$LiMn_4(PO_4)_3$	M+N	26393	1.97	3.78	1.81	-76.64	-74.53	3.37	2	2
$Li_3Mn_2(PO_4)_3$	M+N	849398	1.88	3.78	1.90	-51.91	-41.63	4.11	1	20
$Li_6Mn_9(PO_4)_8$	M+N	25923	1.97	3.78	1.81	-69.51	-65.12	3.13	2	2
$Li_4Mn_7(PO_4)_6$	M+N	849324	1.97	3.78	1.81	-71.05	-67.11	2.98	1	3
$Li_6Mn_3(PO_4)_4$	M+N	780723	1.88	3.78	1.90	-55.39	-48.27	3.37	1	18
$Li_2B_3O_4F_3$	S+N	1196457	1.87	4.44	2.57	-62.11	0	6.57	2	4

$Li_3B_5(HO_5)_2$	S+N	1199091	1.66	3.86	2.20	-3.88	0	5.83	2	6
$Li_{10}B_{14}Cl_2O_{25}$	S+N	23122	1.26	3.52	2.25	-17.02	0	6.40	1	10
$Li_4B_7ClO_1_2$	S+N	1222565	1.37	4	2.62	-21.62	0	5.87	2	4
$Li_2B_4H_4O_9$	S+N	604459	1.91	3.83	1.92	-5.41	0	5.15	1	14
$LiB_3H_3O_5$	S+N	24560	1.91	3.83	1.92	-4.74	0	5.02	4	2

Table S2. Representative 8 crystal structures screened in high-throughput screening process along with their database source, electrochemical window, thermodynamic stability, band gap, and Li – Li networks.

	<i>mp-ID</i>	<i>[V1, V2]</i> <i>ECW</i>	ΔE_{rxn} w/. <i>NCM523</i> (<i>meV</i>)	ΔE_{rxn} w/. <i>LPSC</i> (<i>meV</i>)	<i>Band gap</i> (<i>eV</i>)	<i>N of Li</i> <i>networks</i>	<i>Max N of</i> <i>Li</i> <i>networks</i>
<i>Li₃Sc₂(PO₄)₃</i>	<i>mp-6565</i>	<i>[1.86,</i> <i>4.19]</i> 2.33	-37.30	-24.69	4.76	2	6
<i>LiCaPO₄</i>	<i>mp-16804</i>	<i>[1.17,</i> <i>4.08]</i> 2.91	0	-28.06	5.18	2	3
<i>LiMgPO₄</i>	<i>mp-9625</i>	<i>[1.58,</i> <i>4.18]</i> 2.61	-20.62	0	5.43	2	2
<i>LiH₂ClO</i>	<i>mp-</i> <i>760502</i>	<i>[1.54,</i> <i>4.07]</i> 2.53	0	-22.15	5.31	1	4
<i>Li₃PO₄</i>	<i>mp-13725</i>	<i>[0.69,</i> <i>4.19]</i> 3.51	0	0	5.82	1	6
<i>LiB₃O₅</i>	<i>mp-3660</i>	<i>[1.93,</i> <i>4.22]</i> 2.29	-21.15	0	6.48	2	2
<i>Li₃B₇O₁₂</i>	<i>mp-16828</i>	<i>[1.30,</i> <i>4.22]</i> 2.92	-11.70	0	5.70	2	3
<i>Li₃B₁₁O₁₈</i>	<i>mp-</i> <i>1020014</i>	<i>[1.93,</i> <i>4.41]</i> 2.48	-28.29	0	5.68	2	2

Table S3. Chemical reaction products of 8 representative candidates from the most favorable reactions at NCM523 and LPSC interfaces.

Reaction products		
	NCM523	LPSC
$\text{Li}_3\text{Sc}_2(\text{PO}_4)_3$	$\text{Mn}(\text{Ni}_3\text{O}_4)_2, \text{Ni}_3\text{O}_4, \text{Li}_4\text{MnCo}_5\text{O}_{12},$ $\text{Li}_2\text{Mn}_3\text{NiO}_8, \text{Li}_3\text{PO}_4, \text{Sc}_2\text{O}_3$	$\text{LiScS}_2, \text{Li}_3\text{PS}_4, \text{Li}_3\text{PO}_4, \text{LiCl}$
LiCaPO_4	Stable	$\text{Li}_3\text{PS}_4, \text{Li}_3\text{PO}_4, \text{CaS}, \text{LiCl}$
LiMgPO_4	$\text{Li}_2\text{MgMn}_3\text{O}_8, \text{Ni}_3\text{O}_4, \text{Li}_4\text{MnCo}_5\text{O}_{12},$ $\text{Mg}_6\text{MnO}_8, \text{NiO}, \text{Li}_3\text{PO}_4$	Stable
LiH_2ClO	Stable	$\text{Li}_3\text{PS}_4, \text{Li}_3\text{PO}_4, \text{LiHS}, \text{LiCl}$
Li_3PO_4	Stable	Stable
LiB_3O_5	$\text{LiO}_8, \text{Li}_4\text{MnCo}_5\text{O}_{12}, \text{Li}_2\text{Mn}_3\text{NiO}_8,$ $\text{Ni}_3\text{BO}_5, \text{LiBO}_2$	Stable
$\text{Li}_3\text{B}_7\text{O}_{12}$	$\text{LiO}_8, \text{Li}_4\text{MnCo}_5\text{O}_{12}, \text{Li}_2\text{Mn}_3\text{NiO}_8,$ $\text{Ni}_3\text{BO}_5, \text{LiBO}_2$	Stable
$\text{Li}_3\text{B}_{11}\text{O}_{18}$	$\text{LiO}_8, \text{Li}_2\text{Mn}_3\text{NiO}_8, \text{Ni}_3\text{BO}_5,$ $\text{Co}_3(\text{BO}_3)_2, \text{Li}_3\text{B}_7\text{O}_{12}$	Stable

Table S4. Lattice parameters and energy/atom of $\text{Li}_3\text{Sc}_2(\text{PO}_4)_3$ according to crystal structure phases. The crystal structures are shown in Figure 4(a).

	α -phase	γ -phase
Energy/atom (eV/atom)	-7.205	-7.565
a (Å)	8.8483	8.8290
b (Å)	12.2737	8.7980
c (Å)	8.7959	15.0495
γ (°)	90	125.6
Space group	$P2_1/c$	$P2_1/c$

References

1. SP Ong, Y Mo, WD Richards, L Miara, HS Lee, G Ceder, Phase stability, electrochemical stability and ionic conductivity of the $\text{Li}_{10\pm 1}\text{MP}_2\text{X}_{12}$ ($M = \text{Ge, Si, Sn, Al or P}$, and $X = \text{O, S or Se}$) family of superionic conductors. *Energy Environ. Sci.* 6, 148–156 (2013). doi:10.1039/C2EE23355J.
2. WD Richards, LJ Miara, Y Wang, JC Kim, G Ceder, Interface stability in solid-state batteries. *Chem. Mater.* 28, 266–273 (2016). doi:10.1021/acs.chemmater.5b04082.
3. LJ Miara, WD Richards, YE Wang, G Ceder, First-principles studies on cation dopants and electrolyte|cathode interphases for lithium garnets. *Chem. Mater.* 27, 4040–4047 (2015). doi:10.1021/acs.chemmater.5b01023.